

GAS PERMEABILITY MEASUREMENTS ON SCREENED EVACUATED INSULATION
BASED ON PERFORATED SCREENS

R. S. Mikhal'chenko, V. F. Getmanets,
L. V. Klipach, and P. N. Yurchenko

UDC 536.248.1:536.21

It is shown that the screen perforation parameters influence the transverse gas permeability of the insulation under molecular-flow conditions.

One can reduce the gas pressures in screened evacuated insulation (SEI) by the use of perforated diffraction screens (PDS) [1]. However, difficulties in manufacturing technology have limited their use. A possible way of improving SEI is to optimize the basic parameters of the perforated screens to bring the gas permeabilities up to the level of PDS.

We have examined the transverse gas permeability in SEI containing perforated screens and various inserts as affected by the diameter of the holes (at constant screen porosity) and by the porosity (for a fixed hole diameter). Laboratory methods were used to make specimens whose basic characteristics are given in Table 1.

The permeabilities in the transverse direction were determined by the constant-pressure method under molecular flow conditions with an apparatus that has been described in [2]. The packing densities in all cases were kept constant at 18 screen/cm.

Figure 1 shows that increasing the porosity of screens made from polyethylene terephthalate film aluminized on both sides (DA PET) from 0.5 to 5% at constant hole diameter caused the permeability of the SEI to increase by almost a factor 10. Also, for porosities of 0.5-2%, the diffusion coefficient increases the more rapidly the larger the percent porosity. Locating layers of NT-10 basalt-fiber cloth or glass cloth made from ultrathin fibers type SBSH-T (Fig. 1) between the screens had hardly any effect on the permeability changes (all the curves are described by polynomials of fourth degree), but there is a substantial reduction in the overall permeability. Figure 1 also shows that the permeability of SEI made of perforated DA PET with hole diameter 1.5 mm is reduced by almost a factor 1.5 by the SBSH-T cloth or by 2.5 by NT-10 cloth.

Curves 2 and 4 show that reducing the hole diameter from 1.5 to 1 mm (with constant porosity) increases the diffusion coefficient by a factor 1.5-2 throughout the porosity range because a packing layer density of 18 screen/cm means that the conductivity of the insulation is determined not only by the size of the holes but also by the length of the gaps between the screens, which is equal to the perforation step [2].

Figure 2 shows the effects of hole diameter at constant porosity $\Pi = 3.14\%$. As the diameter decreases, there is a proportional increase in the packet permeability, which applies not only for insulation consisting of perforated screens alone but also for two-component insulation composed of screens and layers (curves 1 and 2).

These permeability measurements agree within 10-30% with calculations from the method of [2].

Elevated gas permeabilities in these packets of perforated screens can thus be provided by reducing the hole diameter to the technically possible minimum while retaining a given porosity. Changing the hole diameter from 2 mm (as used in the ÉVTI-2V commercial insulation screens) to 1 mm increases the diffusion coefficient of the packet with a packing density of 18 screen/cm and porosity 3.14% from 3.9 to 7.3 cm² (Fig. 2, curve 1), which is comparable with the figure for optimized-structure perforated diffraction screens [3], which have porosity 8-9%, hole diameter 0.8 μ m, and film thickness 8 μ m. From $D = (1/4)v_{\alpha}(\Pi_s d_s / 2N)$ we get $D = 5.2-5.8$ cm²/sec for PDS. However, such perforated screens are inferior in degree of black-

Low-Temperature Technical Physics Institute, Academy of Sciences of the Ukrainian SSR, Kharkov. Translated from *Inzhenerno-Fizicheskii Zhurnal*, Vol. 53, No. 1, pp. 87-90, July, 1987. Original article submitted April 1, 1986.

TABLE 1. Characteristics of Perforated Screens Made of DA PET (thickness 10 μm)

Specimen No.	Π_s , %	d_s , mm	l , mm	Specimen No.	Π_s , %	d_s , mm	l , mm
1	0,5	1	12,53	8	1,77	1,5	10
2	1	1	8,86	9	2,54	1,5	8,35
3	1,77	1	6,66	10	3,14	1,5	7,5
4	2,54	1	5,56	11	4	1,5	6,65
5	3,14	1	5	12	5	1,5	5,95
6	0,5	1,5	18,8	13	3,14	2	10
7	1	1,5	13,3	14	3,14	2,5	12,5
				15*	3,14	2	10

*Specimen made of a commercial batch of DA PET film.

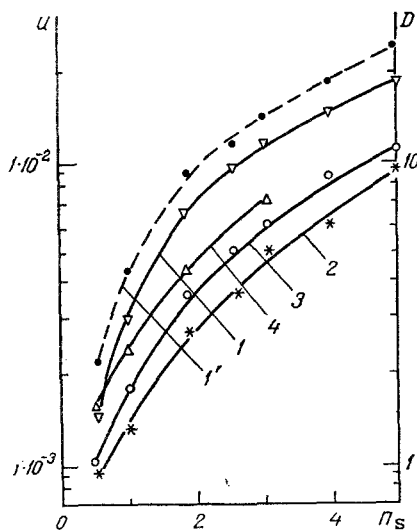


Fig. 1

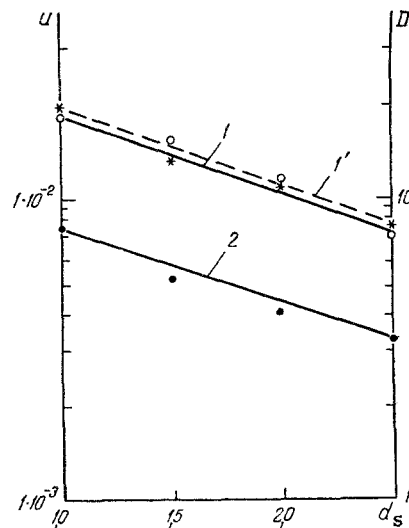


Fig. 2

Fig. 1. Dependence of gas permeability on screen porosity: 1) DA PET, $d_s = 1.5$ mm, $\rho_s = 18$ screen/cm, $\delta_s = 0.01$ mm, $\delta_{pac} = 1$ cm; 2) DA PET, $d_s = 1.5$ mm, $\rho_s = 18$ screen/cm, $\delta_s = 0.01$ mm, and NT-10, $\delta_l = 0.03$ mm, $\delta_{pac} = 1$ cm; 3) DA PET, $d_s = 1.5$ mm, $\rho_s = 18$ screen/cm, $\delta_s = 0.01$ mm and SBSH-T, $\delta_l = 0.03$ mm, $\delta_{pac} = 1$ cm; 4) DA PET, $d_s = 1$ mm, $\rho_s = 18$ screen/cm, $\delta_s = 0.01$ mm and NT-10, $\delta_l = 0.03$ mm, $\delta_{pac} = 1$ cm; 1') theoretical curve; u in liter/($\text{cm}^2 \cdot \text{sec}$), D in cm^2/sec , and Π in %.

Fig. 2. Dependence of gas permeability on hole diameter: 1) DA PET, $\Pi_s = 3.14\%$, $\delta_s = 0.01$ mm, $\rho_s = 18$ screen/cm, $\delta_{pac} = 1$ cm; 2) DA PET, $\Pi_s = 3.14\%$, $\delta_s = 0.01$ mm, $\rho_s = 18$ screen/cm and NT-10, $\delta_l = 0.03$ mm, $\delta_{pac} = 1$ cm; 1') theoretical curve; d in mm.

ness to diffraction ones by factors of 1.35-1.5 [4], so if there are tight specifications for the evacuation rate, one can recommend using perforated PET film with elevated porosity (up to 3.14%) and reduced hole diameter.

NOTATION

D , diffusion coefficient; v_α , thermal velocity; Π_s , screen porosity; d_s , perforation diameter; l , screen thickness; N , number of screens per unit thickness; t , perforation step; δ_s , screen thickness; δ_{pac} , packet thickness; δ_l , interlayer thickness; ρ_s , screen packing density.

LITERATURE CITED

1. R. S. Mikhal'chenko, N. P. Pershin, V. F. Getmanets, et al., *Inzh-Fiz. Zh.*, **45**, No. 6, 902-908 (1983).
2. M. G. Kaganer and Yu. N. Fetisov, *Apparatus and Machines for Oxygen Plant* [in Russian], Issue 14, Moscow (1974), pp. 356-370.

3. R. S. Mikhal'chenko, N. P. Pershin, and L. V. Klipach, Hydrodynamics and Heat Transfer in Cryogenic Systems [in Russian], Kiev (1977), pp. 79-85.
4. N. P. Pershin and R. S. Mikhal'chenko, Heat Transfer at Low Temperatures [in Russian], Kiev (1979), pp. 56-68.

GENERALIZED EQUATION FOR KINETICS OF CONVECTIVE DRYING
OF MOIST MATERIALS

P. S. Kuts, V. Ya. Sklyar,
and A. I. Ol'shanskii

UDC 001.57:685.31.001.5

A generalized equation describing the drying process in continuous-acting convective dryers is derived and analyzed. Results of a numerical solution are compared with experimental data.

An equation was derived in [1] which established the dependence of evaporated moisture output from a convective dryer upon drying time, kinetic characteristics of the process, properties of the material being dried, and flow rate and temperature of the heat-exchange agent. To generalize that study it will be desirable to derive the fundamental equation in dimensionless form, allowing a significant expansion in its practical application range.

The thermal balance equation for a continuous action convective dryer has the form:

$$[\alpha_{cr}(T_h - T_w) + \bar{\alpha}(T_h - T_s)]F = rm_0N + rm_0 \frac{d\bar{u}}{d\tau} + (c_0m_0 + c_m m_m^{11}) \frac{dT_{mt}}{d\tau} \quad (1)$$

Following [1], Eq. (1) can be represented as

$$[St_{cr}(T_h - T_w) + \bar{St}(T_h - T_s)]F = \frac{1}{c_p v \rho} \left[rm_0N + rm_0 \frac{d\bar{u}}{d\tau} + (c_0m_0 + c_m m_m^{11}) \frac{dT_{mt}}{d\tau} \right], \quad (2)$$

where the Stanton numbers St_{cr} and \bar{St} are dimensionless characteristics of the intensity of heat transport in the first and second stages of drying.

The product of two generalized parameters, the relative drying rate N^* and the Rebinder number Rb , can be written in the form

$$N^*Rb = \left(\frac{1}{N} \frac{d\bar{u}}{d\tau} \right) \left(\frac{dT_{mt}}{d\bar{u}} \frac{c_{mt}}{r} \right), \quad (3)$$

while the drying rate in the second stage [2] is given by:

$$\left| \frac{d\bar{u}}{d\tau} \right| = \kappa N (\bar{u} - u_e). \quad (4)$$

It follows from Eqs. (3), (4) that

$$\frac{dT_{mt}}{d\tau} = \frac{r}{c} \kappa N (\bar{u} - u_e) Rb. \quad (5)$$

With consideration of this last relationship, Eq. (2) takes on the form

$$[St_{cr}(T_h - T_w) + \bar{St}(T_h - T_s)]F = \frac{rN}{c_p v \rho} \left[m_0 + m_0 \kappa (\bar{u} - u_e) + (c_0m_0 + c_m m_m^{11}) \frac{\kappa}{c_{mt}} (\bar{u} - u_e) Rb \right]. \quad (6)$$

We will divide both sides of Eq. (6) by the expression $St_{cr}(T_h - T_w) = (T_1 - T_2)f/F$ [3]. With consideration of the expressions [4]

A. V. Lykov Heat and Mass Transfer Institute, Academy of Sciences of the Belorussian SSR, Minsk. Translated from *Inzhenerno-Fizicheskii Zhurnal*, Vol. 53, No. 1, pp. 90-96, July, 1987. Original article submitted April 29, 1986.